The Role of Focal Adhesion Kinase-Phosphatidylinositol 3-Kinase-Akt Signaling in Hepatic Stellate Cell Proliferation and Type I Collagen Expression*

Shimon Reif‡, Alon Lang‡, Jeffery N. Lindquist§, Yutaka Yata‡, Erwin Gäbele‡, Andrew Scanga‡, David A. Brenner‡§, and Richard A. Rippe‡¶

From the ‡Division of Digestive Diseases, Department of Medicine, and the §Department of Biochemistry and Biophysics, University of North Carolina, Chapel Hill, North Carolina 27599

Following a fibrogenic stimulus, the hepatic stellate cell (HSC) undergoes a complex activation process associated with increased cell proliferation and excess deposition of type I collagen. The focal adhesion kinase (FAK)-phosphatidylinositol 3-kinase (PI3K)-Akt signaling pathway is activated by platelet-derived growth factor (PDGF) in several cell types. We investigated the role of the FAK-PI3K-Akt pathway in HSC activation. Inhibition of FAK activity blocked HSC migration, cell attachment, and PDGF-induced PI3K and Akt activation. Both serum- and PDGF-induced Akt phosphorylation was inhibited by LY294002, an inhibitor of PI3K. A constitutively active form of Akt stimulated HSC proliferation in serum-starved HSCs, whereas LY294002 and dominant-negative forms of Akt and FAK inhibited PDGF-induced proliferation. Transforming growth factor-β, an inhibitor of HSC proliferation, did not block PDGF-induced Akt phosphorylation, suggesting that transforming growth factor-β mediates its antiproliferative effect downstream of Akt. Expression of type I collagen protein and α1(I) collagen mRNA was increased by Akt activation and inhibited when PI3K activity was blocked. Therefore, FAK is important for HSC migration, cell attachment, and PDGF-induced cell proliferation. PI3K is positioned downstream of FAK. Signals for HSC proliferation are transduced through FAK, PI3K, and Akt. Finally, expression of type I collagen is regulated by the PI3K-Akt signaling pathway.

Liver fibrosis represents a wound-healing process in response to a variety of chronic stimuli. Fibrosis is characterized by an excessive deposition of extracellular matrix proteins, of which type I collagen predominates. Activation of the hepatic stellate cell (HSC),[1] a perisinusoidal cell that resides in the liver in a quiescent state, is responsible for the increased synthesis and deposition of type I collagen in the liver. Following a fibrogenic stimulus, the HSC undergoes a complex activation process in which the cell changes from a quiescent vitamin A-storing cell to an activated myofibroblast-like cell, which proliferates and becomes fibrogenic (1, 2). An increase in DNA synthesis and cell proliferation occurs with HSC activation. Altered collagen synthesis, at both the mRNA and protein levels, is observed with a dramatic increase in type I collagen and smaller but significant increases in type III and IV collagens (3–5).

Platelet-derived growth factor (PDGF) is the most potent proliferative cytokine for the HSC (1). Liver fibrosis is associated with an increase in PDGF protein expression and increased PDGF receptor expression (6). PDGF receptors contain intrinsic tyrosine kinase activity and, upon binding to its ligand, become autophosphorylated at tyrosine residues (7). PDGF has been shown to transmit proliferative signals in several cell types, including the HSC (8, 9). The activated PDGF receptor acts as a high affinity binding site for several signaling molecules leading to activation of Ras, followed by activation of Raf, MEK, and ERK (10).

Focal adhesion kinase (FAK) has a key role in the synergistic interaction between growth factor and integrin signaling pathways. FAK, a 125-kDa cytoplasmic protein-tyrosine kinase, is a member of the focal adhesion family that mediates integrin-mediated signal transduction leading to a variety of cellular functions, including cell proliferation, migration, and adhesion (11). PDGF induces tyrosine phosphorylation of FAK (12). Association of FAK and phosphatidylinositol 3-kinase (PI3K) is stimulated by PDGF and is required for PDGF stimulation of HSC proliferation (13, 14). Focal adhesion non-kinase (FAK-CD) represents a kinase-deficient splice variant of FAK that contains only the C-terminal portion of FAK and that can inhibit phosphorylation of endogenous FAK, therefore acting as a dominant-negative form of FAK (11, 15).

PI3K represents another key signaling molecule that is recruited to the activated PDGF receptor (16). Activated PI3K generates several phosphoinositols, leading to Akt activation by phosphorylation at Thr[308] and Ser[473] by phosphoinositide-dependent kinase-1 (17). Activated Akt is considered a key downstream survival factor by stimulating cell proliferation and inhibiting apoptosis (17). Akt is activated not only by growth factors that stimulate tyrosine kinase activity, but also by other signals that can activate PI3K, such as integrins and

¶ To whom correspondence should be addressed: Division of Digestive Diseases and Nutrition, Dept. of Medicine, University of North Carolina, CB 7038, Glaxo Bldg., Rm. 134, Chapel Hill, NC 27599. Tel.: 919-966-7469; Fax: 919-966-7468; E-mail: rarippe@med.unc.edu.

[1] The abbreviations used are: HSC, hepatic stellate cell; PDGF, platelet-derived growth factor; MEK, mitogen-activated protein kinase/extracellular signal-regulated kinase kinase; ERK, extracellular signal-regulated kinase; FAK, focal adhesion kinase; PI3K, phosphatidylinositol 3-kinase; FBS, fetal bovine serum; m.o.i., multiplicity of infection; PBS, phosphate-buffered saline; BSA, bovine serum albumin; TBS,

Tris-buffered saline; TGF-β, transforming growth factor-β; STAT, signal transducer and activator of transcription; JNK, c-Jun N-terminal kinase; MAPK, mitogen-activated protein kinase.

stimulators of G-protein-coupled receptors (18–21).

We report here that FAK, PI3K, and Akt are involved in transmitting proliferative signals induced by serum and PDGF in the HSC. We show that both serum and PDGF induce phosphorylation of FAK, PI3K, and Akt and that PI3K and Akt signal downstream of FAK in the HSC. Blocking either FAK or PI3K inhibits HSC adhesion and migration. We demonstrate that PI3K activation is important for both type I collagen mRNA and protein expression in the HSC. Inhibition of PI3K reduces secreted type I collagen protein expression, whereas the intracellular unprocessed collagen intermediates remain unchanged. Therefore, this signaling pathway is critical for HSC proliferation and type I collagen gene expression in the activated HSC.

EXPERIMENTAL PROCEDURES

HSC Isolation and Culture—HSCs were purified from Sprague-Dawley rats (>400 g) by sequential digestion of the liver with Pronase and collagenase, followed by arabinogalactan gradient centrifugation as previously described (22). HSC purity was assessed microscopically and by using the autofluorescence property of the stored retinoids in the HSC. Cell viability was determined by trypan blue exclusion staining. HSC populations were consistently found to be between 90 and 99% pure and 95% viable. HSCs were cultured on plastic in Dulbecco's modified Eagle's medium (Invitrogen) supplemented with 10% fetal bovine serum (FBS) and 2 mM L-glutamine in a 95% air and 5% CO_2 humidified atmosphere. HSCs were activated by culturing on plastic for 7–14 days. The purity of culture-activated HSCs was assessed by immunohistochemistry using mouse anti-human smooth muscle α-actin (Dako Corp., Carpinteria, CA).

Adenoviral Transduction of HSCs—Ad5LacZ, which contains the β-galactosidase gene driven by the cytomegalovirus promoter, was used as a control virus throughout this study. The Ad5FAK-CD virus contains the dominant-negative form of FAK (23). The Ad5myrAkt and Ad5dnAkt viruses express activated and dominant-negative forms of Akt, respectively (24, 25). Quiescent HSCs, 1 day after isolation (day 1), were infected with Ad5FAK-CD or Ad5LacZ at a multiplicity of infection (m.o.i.) of 500 for 12 h in Dulbecco's modified Eagle's medium containing 10% FBS. After infection, the medium was changed to fresh growth medium. For proliferation and apoptosis studies, culture-activated HSCs (day 15) were infected at m.o.i. = 500 in medium containing 0.2% FBS. After 12 h, the medium was changed to fresh medium containing 0.2% FBS, and the cells were incubated for an additional 24 h prior to performing the individual experiments.

Immunostaining—HSCs were seeded onto glass coverslips and infected with AdFAK-CD at m.o.i. = 500. After 24 h of infection, the coverslips were washed twice with cold phosphate-buffered saline (PBS), and the cells were fixed and permeabilized with cold methanol for 8 min. The methanol was removed, and the coverslips were air-dried at room temperature. Immunostaining was performed using the Dako Envision system peroxidase staining kit as directed by the manufacturer. Coverslips were washed once with PBS containing 0.2% Tween 20 and then incubated with peroxidase-blocking reagent at room temperature for 5 min. Coverslips were gently washed with PBS containing 0.2% Tween 20 and subsequently incubated with anti-hemagglutinin antibody (Roche Molecular Biochemicals) at a 1:200 dilution in PBS and 1% bovine serum albumin (BSA) at room temperature for 10 min. Coverslips were washed and incubated with the peroxidase-labeled polymer at room temperature for 10 min and washed as described above. The substrate/chromogen solution was prepared according to the manufacture's protocol and incubated on the coverslips at room temperature for 10 min, and the slides were washed with water. The 3,3-diamino benzidine/enhancer solution was added, incubated at room temperature for 5 min, and then washed with water. The coverslips were counterstained with hematoxylin for 30 s, rinsed well with water, and dried for 10 min. The slides were dehydrated with two 100% ethanol washes for 20 s each and finally with xylene for 20 s. The coverslips were mounted onto glass slides and viewed microscopically.

Analysis of DNA Synthesis—DNA synthesis was assessed by [³H]thymidine incorporation. This assay was used to assess cell proliferation, as cell counts correlated with the results of the [³H]thymidine incorporation assay (data not shown). Culture-activated HSCs (7–10 days in culture) were seeded at a density of 2×10^4 cells/well in 24-well plates in growth medium containing 10% FBS. After 24 h, the medium was changed to 0.2% FBS, and the cells were infected with either Ad5FAK-CD or Ad5LacZ at m.o.i. = 500. The medium was changed after 12 h to medium containing 0.2% FBS, and the cells were incubated for an additional 24 h. Afterward, the cells were incubated in medium containing 10 ng/ml human PDGF-BB (Roche Molecular Biochemicals) for 48 h with 1 μCi/ml [³H]thymidine present during the last 24 h. At the end of the incubation, 10% trichloroacetic acid was added, and the cells were maintained on ice for 15 min. Cells were washed twice with cold 10% trichloroacetic acid and solubilized in 0.2 N NaOH, and radioactivity was measured using a scintillation counter. Each experiment was performed in quadruplicate and repeated at least three times.

Cell Migration Assay—Cell migration was assessed by measuring the repair of a linear wound generated in a confluent monolayer of HSCs (26). Parallel lines were drawn on the bottom of wells before plating the cells. A linear wound was generated in the monolayer of cells by scraping a sterile plastic pipette tip perpendicular to the lines. The distance between the wound and cell front was measured with a micrometer, using the lines on the bottom of the well as a reference, immediately after creating the wound and 24 h later. Activated HSCs were uninfected, infected with the Ad5LacZ or Ad5FAK-CD virus for 24 h before generating the wound, or treated with the PI3K inhibitor 25 μM LY294002 (Calbiochem) or vehicle (Me₂SO) 30 min before generating the wound. To assure that wound closure represents migration and not cell proliferation, HSCs were treated with 2.5 μg/ml mitomycin C 2 h before creating the wound.

Cell Adhesion Assay—Culture-activated HSCs were uninfected, infected with the Ad5LacZ or AdFAK-CD virus, or treated with 25 μM LY294002 or Me₂SO. Twenty-four hours after infection or 30 min after LY294002 or Me₂SO treatment, HSCs were detached from the culture dishes with trypsin, and the detached cells were suspended in Dulbecco's modified Eagle's medium containing 10% FBS. The cells were replated on tissue culture dishes. Two hours after replating, the cells were washed twice with PBS to remove unattached cells, and the adherent cells were trypsinized and counted.

FAK Immunoprecipitation and Western Blotting—HSCs were lysed with radioimmune precipitation assay buffer (50 mM Tris-HCl (pH 8.0), 150 mM NaCl, 1% Nonidet P-40, 0.5% sodium deoxycholate, 0.1% SDS, 1 mM Na₃VO₄, 10 μg/ml aprotinin, and 10 μg/ml leupeptin). The lysate was centrifuged at 4 °C for 10 min, and protein concentration was determined using the Bradford method (Bio-Rad). Cell lysate (250 μg) was incubated with 30 μl of anti-FAK antibody (specific for the N terminus of FAK) and with protein A/G-Sepharose beads (Santa Cruz Biotechnology, Santa Cruz, CA) at 4 °C for 3 h. The beads were washed three times with radioimmune precipitation assay buffer, boiled for 5 min in SDS buffer, and applied to standard 10% SDS-polyacrylamide protein gel. After electrophoresis, the proteins were electrophoretically transferred onto nitrocellulose membranes (Schleicher & Schüll) using a Transblot apparatus in buffer containing 20 mM glycine and 20% methanol. The membrane was stained with 0.5% Ponceau S to assure equal loading of the gel and transfer of the proteins. The membrane was blocked with 3% BSA in Tris-buffered saline (TBS; 25 mM Tris-HCl (pH 8.0) and 144 mM NaCl) containing 0.1% Tween 20 (TBS-T) at room temperature for 45 min. Afterward, the membrane was incubated with the primary antibody: anti-FAK polyclonal antibody (Santa Cruz Biotechnology) diluted 1:1000 in 1% BSA in TBS-T or anti-phosphotyrosine monoclonal antibody (Transduction Laboratories, Lexington, KY) diluted 1:2000 in 1% BSA in TBS-T at room temperature for 45 min. The membrane was washed five times with TBS-T and incubated with horseradish peroxidase-conjugated anti-goat or goat anti-mouse antibody (Amersham Biosciences) diluted 1:5000 in 1% BSA in TBS-T at room temperature for 30 min. The membrane was washed five times with TBS-T, and signals were detected using the ECL Western blot detection system kit (Amersham Biosciences) according to the manufacturer's recommended protocol.

PI3K Assay—Culture-activated HSCs were lysed in buffer containing 20 mM Tris-HCl (pH 7.5), 150 mM NaCl, 2 mM EDTA, 1% sodium deoxycholate, 1% Triton X-100, and 0.25% SDS. The cell lysate (500 μg) was incubated overnight at 4 °C with anti-PI3K p110β antibody (Santa Cruz Biotechnology). Antigen-antibody immune complexes were captured with protein A/G-Sepharose beads at 4 °C for 2 h. The beads were washed three times with 1% Nonidet P-40 and 100 μM Na₃VO₄ in PBS; twice with 100 mM Tris-HCl (pH 7.5), 500 mM LiCl, and 100 μM Na₃VO₄; and twice with 100 mM Tris-HCl (pH 7.5), 100 mM NaCl, 1 mM EDTA, and 100 μmol/liter Na₃VO₄. The beads were centrifuged at $16,000 \times g$ for 1 min at room temperature and suspended in 50 μl of 10 mM Tris-HCl (pH 7.5), 100 mM NaCl, and 1 mM EDTA and 10 μl of 10 mM MgCl₂ to which 10 μl of a 2 μM solution of phosphatidylinositol (Avanti, Pelham, AL) was added. The reaction was initiated by adding 5 μl of 440 μM ATP and 15 μl of [³²P]ATP (3000 Ci/ml), and the reaction

mixture was incubated at 22 °C for 10 min. The reaction was stopped by the addition of 20 μl of 8 N HCl and 160 μl of chloroform/methanol (1:1). After centrifugation at $16,000 \times g$ for 10 min at room temperature, the lower phase was applied to TLC plates coated with 1% potassium oxalate, and the reaction products were separated in a TLC chamber containing chloroform/methanol/water/ammonium hydroxide (60:47:11.3:2) buffer. Following chromatography, the TLC plate was subjected to autoradiography to visualize the phosphorylated substrate.

Western Blot Analysis—Cultured HSCs were washed with PBS, and the cells were lysed with protein sample buffer (100 mM Tris-HCl (pH 6.8), 200 mM dithiothreitol, 4% SDS, 0.2% bromphenol blue, and 20% glycerol). Protein concentrations were measured using the Bradford method. Protein samples were heated at 95 °C for 5 min, and 20 μg was applied to a 10% SDS-polyacrylamide gel (7.5% SDS-polyacrylamide gels were used for collagen analysis). After electrophoresis, the proteins were electrophoretically transferred onto nitrocellulose membranes. Membranes were stained with 0.5% Ponceau S to assure equal protein loading and transfer. The membrane was blocked for 1 h with 5% powdered milk in TBS-T. Afterward, the membrane was incubated with the primary antibody: anti-phospho-Ser[473] Akt or anti-total Akt polyclonal antibody (New England Biolabs Inc., Beverly, MA) diluted 1:1000 in 5% milk in TBS-T or anti-type I collagen polyclonal antibody (Rockland Inc., Gilbertsville, PA). The membrane was washed four times with TBS-T for 15 min each wash and then incubated with horseradish peroxidase-conjugated goat anti-rabbit IgG antibody diluted 1:1000 for Akt and 1:5000 for collagen in 5% milk in TBS-T. The membrane was washed five times with TBS-T for 10 min each wash. Immunodetected proteins were visualized using the ECL assay kit.

RNase Protection Assay—RNase protection assays were performed as described previously (27). Radiolabeled probes were prepared for rat $\alpha1(I)$ collagen (27) and glyceraldehyde-3-phosphate dehydrogenase (pTRI-GAPDH-Rat, Ambion Inc., Austin, TX) and mixed with 5 μg of total RNA. Protected fragments were analyzed on standard 6% sequencing gels. Following electrophoresis, bands were visualized by autoradiography and quantitated by PhosphorImager analysis (Amersham Biosciences).

Analysis of Type I Collagen Protein Expression—Proteins from the culture medium were precipitated by the addition of ammonium sulfate to 40% at 4 °C. Samples were centrifuged at $10,000 \times g$ for 30 min at 4 °C, and the pellet was suspended in 0.5 M acetic acid. Aliquots of the protein sample were digested with 130 units of pepsin (Sigma), neutralized with 1.5 M Tris-HCl (pH 8.8), and digested with 8 units of collagenase (Sigma), or protein sample buffer was added. Digestion reactions were performed at room temperature for 30 min. Samples were applied onto a 7.5% polyacrylamide gel, and Western blot analysis was performed for type I collagen as described above.

RESULTS

Ad5FAK-CD Infection Inhibits FAK Phosphorylation—Because homozygous FAK knockout mice are embryonic lethal (28), we needed to develop a novel strategy to assess the role of FAK in HSCs. To evaluate the effects of blocking FAK in activated HSCs, culture-activated rat HSCs were transduced with Ad5FAK-CD expressing a dominant-negative form of FAK (23). The cells were immunostained 24 h after transduction for the hemagglutinin epitope present on the FAK-CD protein. At m.o.i. = 500, >90% of the cells expressed the hemagglutinin-tagged FAK-CD protein (data not shown). To determine whether the dominant-negative FAK-CD protein effectively inhibits FAK phosphorylation, culture-activated HSCs were transduced with either Ad5FAK-CD or control Ad5LacZ. Total cell protein was harvested 48 h after infection and immunoprecipitated with anti-FAK antibody (recognizing the N-terminal portion of FAK). Immunoprecipitated complexes were subjected to SDS-PAGE, followed by immunoblotting for anti-FAK or anti-phosphotyrosine antibody. The FAK-CD protein effectively reduced the level of endogenous FAK protein in activated HSCs and inhibited the level of phosphorylated endogenous FAK (Fig. 1). The dual effects of down-regulating both FAK protein levels and FAK phosphorylation by FAK-CD have been observed in other cell types (23).

Blocking FAK or PI3K Inhibits PDGF-stimulated DNA Synthesis in the HSC—To determine whether FAK has a role in
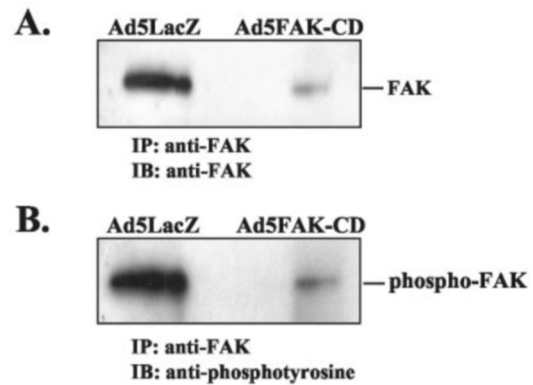
FIG. 1. **FAK-CD reduces the level of FAK protein and the level of phosphorylated FAK in HSCs.** HSCs were transduced with the control Ad5LacZ virus, which expresses β-galactosidase, or with Ad5FAK-CD (m.o.i. = 500). Extracts of total cell proteins were immunoprecipitated (*IP*) with anti-FAK antibody (recognizing only the N-terminal portion of the protein). The immunoprecipitated protein was separated by SDS-PAGE, followed by immunoblotting (*IB*) for anti-FAK (*A*) or anti-phosphotyrosine (*B*) antibody.
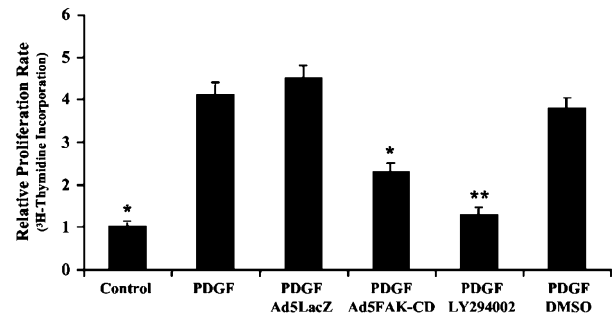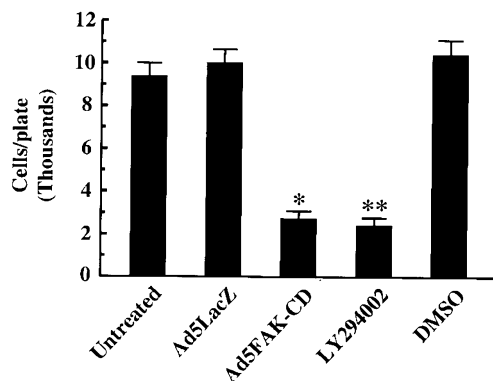

FIG. 2. **Blocking FAK inhibits proliferation of HSCs.** Culture-activated HSCs were left untreated or were infected with Ad5LacZ or Ad5FAK-CD or treated with 25 μM LY294002 or Me$_2$SO (*DMSO*). Cells were cultured in 0.2% serum to inhibit cell proliferation. Following 24 h of serum starvation, the cells were stimulated to proliferate with 20 ng/ml PDGF for 48 h. During the last 24 h of incubation, 1 $\mu Ci/ml$ [^{3}H]thymidine was added. Control cells were maintained in 0.2% serum. Data represent three independent experiments, each performed in quadruplicate. *, $p < 0.01$ *versus* rates in Ad5LacZ-infected HSCs; **, $p < 0.01$ *versus* rates in Me$_2$SO-treated HSCs.

cell proliferation in culture-activated HSCs, we assessed [^{3}H]thymidine incorporation following Ad5FAK-CD transduction. Following Ad5FAK-CD transduction and a 24-h period of serum starvation, HSC proliferation was stimulated with 20 ng/ml PDGF-BB. Ad5FAK-CD inhibited DNA synthesis in culture-activated HSCs by 49 ± 0.2% (Fig. 2). Because PI3K is a common downstream target of FAK, we assessed the role of PI3K in PDGF-induced HSC proliferation. Culture-activated HSCs were serum-starved for 24 h and then treated with 25 μM LY294002, a specific pharmacological inhibitor of PI3K, or vehicle (Me$_2$SO). Cells were treated with LY294002 for 1 h and then stimulated with 20 ng/ml PDGF-BB. LY294002 treatment blocked DNA synthesis by 70.2 ± 0.17% in culture-activated HSCs compared with control cells.

FAK and PI3K Are Important for HSC Adhesion and Cell Migration—FAK is involved in cell adhesion (11). To determine the role of FAK in adhesion of HSCs, we assayed HSC attachment after trypsinizing and replating the cells following Ad5FAK-CD transduction. Blocking FAK with the FAK-CD protein inhibited HSC adhesion by 72.6 ± 3.7% (Fig. 3*A*). Treating the cells with 25 μM LY294002 also inhibited cell attachment by 76 ± 4.0% (Fig. 3*A*).

Cell migration of culture-activated HSCs was assessed by measuring the repair of a linear wound generated in a conflu-

A.

B.
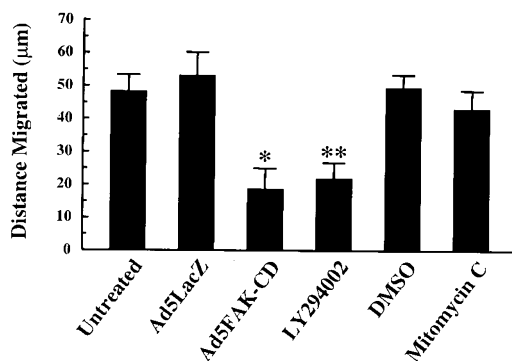
FIG. 3. **Blocking FAK or PI3K inhibits adhesion and migration of HSCs.** *A*, to assess cell attachment, culture-activated HSCs were left untreated, infected with Ad5LacZ or Ad5FAK-CD, or treated with 25 μM LY294002 or Me$_2$SO (*DMSO*). Twenty-four hours after viral infection or 30 min after LY294002 or Me$_2$SO treatment, HSCs were detached from culture dishes with trypsin. The detached cells were suspended in Dulbecco's modified Eagle's medium containing 10% FBS and then replated on tissue culture dishes. Two hours after replating, the cells were washed twice with PBS to remove unattached cells, trypsinized, and counted. Data represent three independent experiments, each performed in quadruplicate. *, $p < 0.01$ *versus* Ad5LacZ-infected HSCs; **, $p < 0.01$ *versus* Me$_2$SO-treated HSCs. *B*, cell migration was assessed by measuring the repair of a linear wound generated in a confluent monolayer of culture-activated HSCs. The distance cells migrated from the front of the wound was measured using a micrometer immediately after generating the wound and 24 h later. Culture-activated HSCs were left untreated, infected with Ad5LacZ or Ad5FAK-CD for 24 h prior to creating the wound, or treated with the PI3K inhibitor 25 μM LY294002 or its vehicle (Me$_2$SO) 30 min prior to creating the wound. Both Ad5FAK-CD and the PI3K inhibitor prevented migration of culture-activated HSCs. Data represent three independent experiments, each performed in triplicate. *, $p < 0.01$ *versus* Ad5LacZ-transduced HSCs; **, $p < 0.01$ *versus* Me$_2$SO-treated HSCs.

ent monolayer of activated HSCs. Culture-activated HSCs were transduced with Ad5FAK-CD prior to generating the wound in a cell monolayer. Blocking FAK activity inhibited migration of HSCs by $64.7 \pm 8.2\%$ compared with transduced control cells (Fig. 3*B*). Incubation of culture-activated HSCs with 25 μM LY294002 also inhibited cell migration by $58.7 \pm 9.4\%$ compared with cells treated with vehicle (Me$_2$SO) (Fig. 3*B*). To assure that wound closure represents cell migration and not a proliferative response, HSCs were treated with 2.5 μM mitomycin C, an inhibitor of cell proliferation, 2 h prior to generating the wound. Treatment of the cells with mitomycin C did not affect wound closure, thus demonstrating that the response measured cell migration and not cell proliferation.
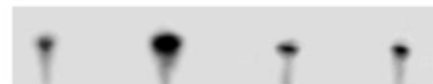
FIG. 4. **PI3K signals downstream of FAK.** Culture-activated HSCs were infected with the control Ad5LacZ virus or with Ad5FAK-CD. Total cell proteins were immunoprecipitated with anti-PI3K p110β antibody. Immunoprecipitates were assayed for PI3K activity by phosphorylation of phosphatidylinositol in the presence of [^{32}P]ATP, and phosphorylated products were detected by TLC, followed by autoradiography. Data are representative of two separate experiments.

Together, these data show that blocking either FAK or PI3K inhibits cell adhesion and migration of HSCs.

PI3K Signals Downstream of FAK in the Activated HSC— Inhibiting FAK or PI3K results in similar effects on HSC DNA synthesis, cell adhesion, and cell migration, suggesting that these signaling molecules are jointly involved in the cellular signaling cascade meditating these cellular events. Therefore, we wanted to determine whether PI3K acts downstream of FAK in HSC signaling. Culture-activated HSCs were transduced with either Ad5FAK-CD or Ad5LacZ or treated with 25 μM LY294002. The cells were subsequently serum-starved to reduce their proliferation rate and then induced to proliferate with 20 ng/ml PDGF-BB. Total cell protein was immunoprecipitated with anti-PI3K antibody, and PI3K assays were performed. The control Ad5LacZ virus did not affect PI3K activity; however, infection with Ad5FAK-CD markedly inhibited PI3K activity (Fig. 4). These data demonstrate that PI3K acts downstream of FAK in PDGF-stimulated HSC signaling.

Akt Phosphorylation Is Induced by Serum and PDGF in HSCs— Akt has been implicated as a signaling molecule in several cell types and is positioned downstream of PI3K. Because both serum and PDGF stimulated HSC proliferation, we assessed whether serum and PDGF can induce Akt phosphorylation. Culture-activated HSCs were serum-starved for 48 h and pretreated for 1 h with 25 μM LY294002 prior to treatment with either 10% serum or 20 ng/ml PDGF-BB. Cells were harvested 10, 20, 30, and 60 min following stimulation, and Akt phosphorylation status was assessed by Western blot analysis. Within 10 min of serum (Fig. 5*A*) or PDGF-BB (Fig. 5*B*) stimulation, phosphorylation of Akt at Ser^{473} was observed, indicating Akt activation. Interestingly, Akt phosphorylation levels began to diminish 60 min following serum stimulation. Pretreatment of the cells with 25 μM LY294002 completely inhibited both serum- and PDGF-induced Akt phosphorylation at each time point. To assure equal protein loading, total Akt levels were assessed and found to be similar (Fig. 5).

Akt Transmits Proliferative Signaling in HSCs— To assess the role of Akt in HSC proliferation, culture-activated HSCs were either transduced with Ad5myrAkt or Ad5dnAkt or treated with LY294002. Afterward, the cells were serum-starved for 48 h and then stimulated to proliferate with 10% serum. The dominant-negative form of Akt and LY294002 treatment inhibited serum-induced HSC DNA synthesis by 72.6 and 92.7%, respectively (Fig. 6). Overexpression of the constitutively active form of Akt stimulated HSC DNA synthesis to levels equal to 10% serum (Fig. 6). LY294002 treatment markedly inhibited HSC DNA synthesis. Cell counts (data not shown) showed similar results, indicating that PI3K and Akt are involved in transmitting proliferative signals in the HSC.

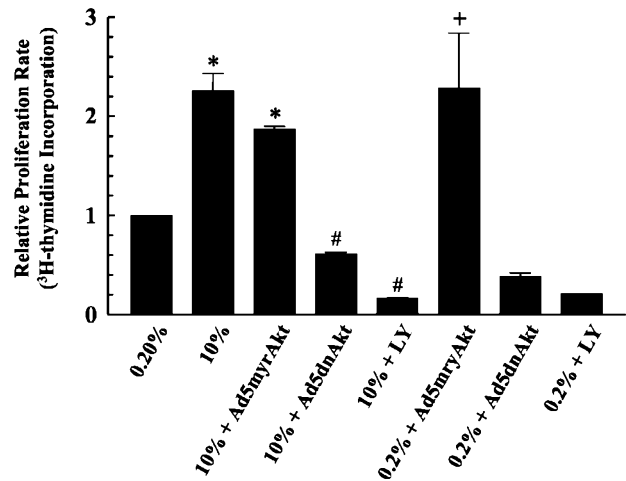*Akt Signals Downstream of FAK in PDGF-stimulated Activated HSCs—* Because we demonstrated that PI3K signals
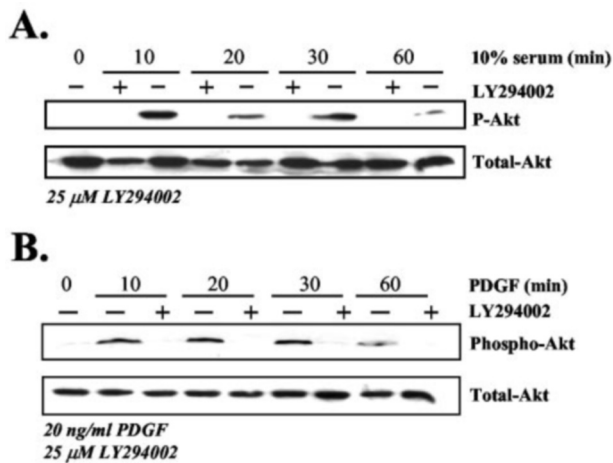
FIG. 5. **LY294002 inhibits serum- and PDGF-induced Akt phosphorylation.** Activated HSCs were serum-starved for 48 h and then treated with 25 μM LY294002 for 1 h. Serum (10% final concentration) (*A*) or 20 ng/ml PDGF-BB (*B*) was added to the cells for 0, 10, 20, 30, and 60 min. Total cell protein was harvested, and Western blot analysis was performed using anti-phospho-Ser[473] Akt (*P-Akt*; *upper panels*) or anti-total Akt (*lower panels*) polyclonal antibody. Equal loading of the gels was confirmed by Ponceau S staining of the transfer membrane (data not shown).

FIG. 6. **Akt stimulates HSC DNA synthesis.** Culture-activated HSCs were transduced with Ad5myrAkt or Ad5dnAkt. Cells were serum-starved (0% serum) for 48 h to reduce the proliferation rate of the cells. Proliferation was induced with 10% serum, and DNA synthesis was assessed by [³H]thymidine incorporation. Cells were treated with 25 μM LY294002 (*LY*) for 1 h prior to the addition of serum. Data represent the average values obtained from two to eight different experiments, each performed in quadruplicate. *Error bars* represent S.E. Statistical analysis using the Mann-Whitney rank sum test showed the following: *, $p < 0.05$ compared with 0.2% serum; #, $p < 0.05$ compared with 10% serum; +, $p < 0.05$ compared with 0.2% serum.
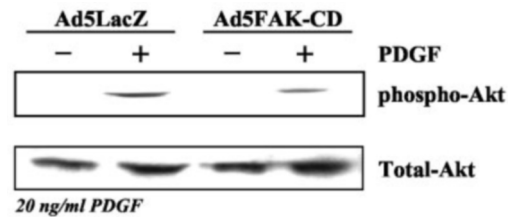
FIG. 7. **Blocking FAK activity inhibits PDGF-induced Akt phosphorylation.** Culture-activated HSCs were transduced with Ad5LacZ or Ad5FAK-CD; and 24 h later, the cells were serum-starved for 48 h. Cells were subsequently treated with or without 20 ng/ml PDGF for 20 min. Total cell proteins were harvested, and Western blot analysis was performed using anti-phospho-Ser[473] Akt (*upper panel*) or total Akt (*lower panel*) polyclonal antibody. Equal loading of the gel was confirmed by Ponceau S staining of the transfer membrane (data not shown). Densitometric analysis demonstrated a 37% reduction in phospho-Akt levels in cells transduced with Ad5FAK-CD compared with cells transduced with Ad5LacZ when normalized to total Akt levels. Data are representative of two separate experiments.

downstream of FAK (Fig. 4), we wanted to determine whether Akt also signals downstream of FAK following PDGF-induced stimulation in activated HSCs. Culture-activated HSCs were transduced with either Ad5FAK-CD or Ad5LacZ. The cells were serum-starved to reduce their proliferation rate. After 48 h, the cells were induced to proliferate with 20 ng/ml PDGF-BB. Cells were harvested after 20 min of PDGF stimulation, and Western blot analysis was performed for phospho-Akt. The control Ad5LacZ virus did not affect PDGF-induced phosphorylation of Akt; however, infection with Ad5FAK-CD inhibited PDGF-induced Akt phosphorylation by 37% (Fig. 7). No changes were observed in total Akt levels (Fig. 7). These data demonstrate that Akt signals downstream of FAK in PDGF-stimulated HSC signaling.

Transforming Growth Factor-β (TGF-β) Does Not Inhibit PDGF-induced Akt Phosphorylation—TGF-β has previously been shown to inhibit HSC proliferation (29, 30). We wanted to determine whether TGF-β inhibits HSC proliferation at the level of Akt phosphorylation following PDGF stimulation. Culture-activated HSCs were serum-starved for 48 h and then treated under five different conditions: 1) 5 ng/ml TGF-β for 1 h, 2) 20 ng/ml PDGF for 20 min, 3) 5 ng/ml TGF-β for 1 h and then 20 ng/ml PDGF for 20 min, 4) 5 ng/ml TGF-β together with 20 ng/ml PDGF for 20 min, and 5) pretreatment with 20 ng/ml PDGF for 10 min prior to treatment with 5 ng/ml TGF-β. TGF-β treatment alone failed to stimulate Akt phosphorylation and did not inhibit PDGF-induced phosphorylation of Akt when added prior to, at the same time as, or after PDGF stimulation (Fig. 8). Total Akt levels were equal at all points, showing equal loading of the gel (Fig. 8). Therefore, TGF-β must exert its antiproliferative effects downstream of Akt in HSCs.

Blocking PI3K Activity Inhibits α1(I) Collagen Expression—To assess whether PI3K is involved in regulating α1(I) collagen gene expression, culture-activated HSCs were treated with 25 μM LY294002 for 24, 48, and 72 h in the presence of 10% serum, and α1(I) collagen mRNA levels were assessed by RNase protection assays. After 24 h of LY294002 treatment, no significant reduction in α1(I) collagen mRNA levels was detected; however, α1(I) collagen mRNA levels were reduced to 46.6 and 27.4% of control Me$_2$SO-treated cells after 48 and

72 h, respectively (Fig. 9). Type I collagen protein levels were also examined in cell extracts and in the culture medium (Fig. 10*A*). LY294002 treatment did not reduce intracellular type I collagen protein processing intermediates during the 72-h treatment. However, secreted type I collagen protein levels were markedly reduced after 24 and 48 h of LY294002 treatment and were essentially undetected after 72 h of LY294002 treatment (Fig. 10*A*). As expected, only processing intermediates of type I collagen were detected intracellularly as assessed by pepsin digestion, which cleaves the N- and C-propeptides off the mature collagen triple-helical molecule (Fig. 10*B*). Digestion with collagenase completely degraded the protein bands, showing that they represent collagen proteins (Fig. 10*B*).

Akt Regulates α1(I) Collagen mRNA Expression—To investigate whether Akt regulates type I collagen expression, culture-activated HSCs were transduced with Ad5myrAkt or Ad5dnAkt. As a control, cells were either uninfected or transduced with Ad5LacZ. HSCs transduced with Ad5myrAkt showed a 2.3-fold increase in α1(I) collagen mRNA expression compared with control cells or cells transduced with either
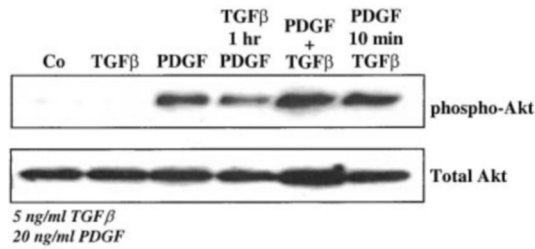
FIG. 8. **TGF-β fails to inhibit PDGF-induced Akt phosphorylation.** Culture-activated HSCs were serum-starved for 48 h. Cells were treated under five conditions: 1) 5 ng/ml TGF-β for 1 h, 2) 20 ng/ml PDGF for 20 min, 3) 5 ng/ml TGF-β for 1 h and then 20 ng/ml PDGF for 20 min, 4) 5 ng/ml TGF-β together with 20 ng/ml PDGF for 20 min, and 5) 20 ng/ml PDGF for 10 min and then 5 ng/ml TGF-β for 10 min. Total cell proteins were harvested, and Western blot analysis was performed using anti-phospho-Ser[473] Akt (*upper panel*) or total Akt (*lower panel*) polyclonal antibody. Equal loading of the gel was confirmed by Ponceau S staining of the transfer membrane (data not shown). *Co*, control.
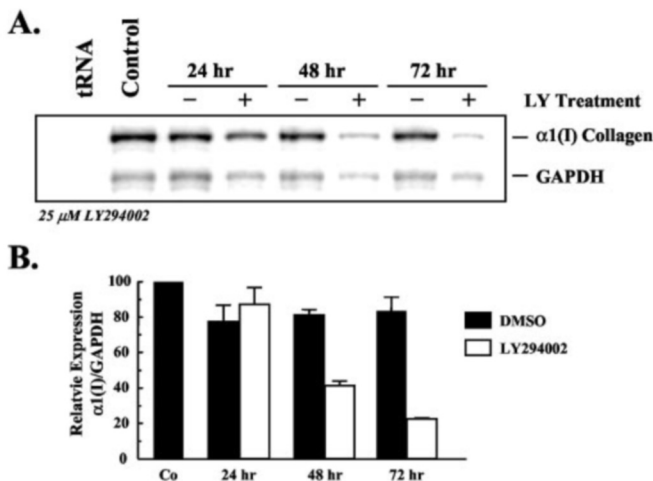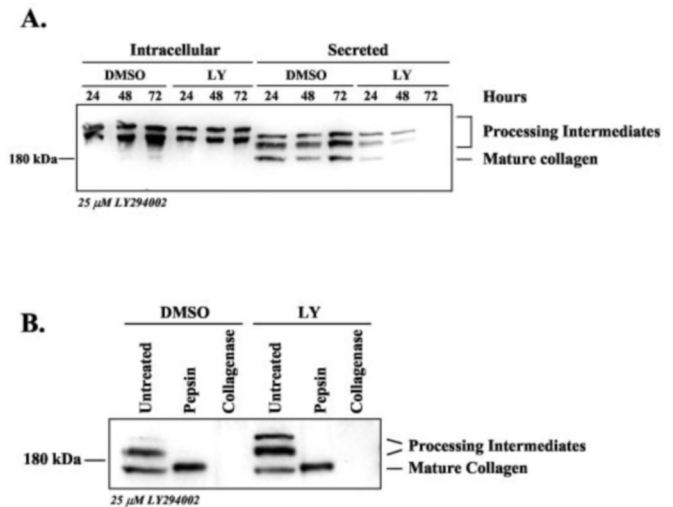

FIG. 9. **Inhibition of PI3K inhibits α1(I) collagen mRNA expression.** *A*, culture-activated HSCs were treated with 25 μM LY294002 (*LY*) or Me₂SO (*DMSO*) for 24, 48, and 72 h, and total RNA was harvested. RNase protection assays were performed to assess the levels of α1(I) collagen. Expression of α1(I) collagen mRNA is expressed relative to glyceraldehyde-3-phosphate dehydrogenase (*GAPDH*). Representative RNase protection assay results are shown. The *Control lane* represents RNA from untreated culture-activated HSCs, and tRNA was also used in the assay as a negative control RNA sample. *B*, a graphical analysis of the RNase protection assay data is shown. Data represent results from two to four individual RNase assays. *Error bars* represent S.E. *Co*, control.

Ad5LacZ or Ad5dnAkt (Fig. 11*A*). The levels of intracellular type I collagen protein were also increased by Ad5myrAkt, whereas no effect on type I collagen protein levels were observed in cells transduced with the control Ad5LacZ adenovirus or Ad5dnAkt (Fig. 11*B*). No difference in the expression of smooth muscle α-actin protein levels, a standard measure of HSC activation, was detected (data not shown).

DISCUSSION

Two major events occur following HSC activation that promote the fibrogenic response of these cells. First, HSCs change their pattern of gene expression, increasing the synthesis and deposition of extracellular matrix proteins and especially that of type I collagen; hence, these cells become directly fibrogenic. Second, the proliferation rate of HSCs increases, thereby effectively amplifying the number of fibrogenic cells present in the liver. Therefore, it is believed that effective treatment regimes aimed at reducing or inhibiting either the fibrogenic or proliferative responses of HSCs would reduce the deleterious effects of HSCs in the progression of fibrosis.


FIG. 10. **Inhibition of PI3K inhibits secreted type I collagen protein expression, but does not affect intracellular levels of type I collagen protein.** *A*, HSCs were culture-activated, and total cell protein and proteins obtained from the culture medium were treated for 24, 48, or 72 h with 25 μM LY294002 (*LY*) or Me₂SO (*DMSO*) as a control. Proteins were subjected to Western blot analysis for type I collagen expression. *B*, to assess the identity of the different bands detected, protein samples from the 24-h time points were subjected to either pepsin or collagenase digestion. Pepsin reduced the two upper bands to the lower band, indicating that the upper bands contain the N-and/or C-terminal propeptides and showing that the lower band represents mature type I collagen. Collagenase digestion eliminated all bands, indicating that all bands represent collagen.

PDGF is the most potent mitogenic factor for HSC proliferation (1). Several signaling pathways have been described that regulate HSC proliferation involving cross-talk between the different signaling pathways (Fig. 12). PDGF treatment of HSCs activates Ras, followed by the sequential activation of Raf, MEK, and ERK in HSCs (6, 10, 32). Activation of ERK is observed following PDGF stimulation in culture-activated HSCs and in HSCs isolated from animals treated with a single dose of CCl₄ (33). PDGF-induced ERK activation in human HSCs is followed by transient up-regulation of c-*fos* expression and AP-1 and STAT1 binding activities (34, 35). Blocking ERK activity with the pharmacological inhibitor PD98059 inhibits HSC proliferation along with AP-1 and STAT1 DNA-binding activities, thus supporting a role for ERK activation in HSC proliferation (33).

c-Jun and JNK are positive regulators of cell proliferation in several cell types, including HSCs (36–38). Blocking JNK activity in quiescent HSCs or in culture-activated HSCs with a dominant-negative form of JNK prevents cell proliferation (38). Interestingly, inhibition of p38 MAPK in either quiescent or activated HSCs with the pharmacological inhibitor SB203580 actually increases cell proliferation, implying that activation of p38 inhibits HSC proliferation (38). An inhibitory role for p38 in cell proliferation has been shown in other cell types, perhaps by inhibiting cyclin D1 (39). Indeed, culture-induced proliferation of HSCs is associated with increased mRNA and protein levels of cyclins D1, D2, and E (40).

PDGF also activates FAK, a member of the focal adhesion complex family (12). This complex interacts with extracellular matrix proteins through integrin interactions, providing a direct sensor to the integrity and composition of the extracellular environment. Following integrin activation, FAK is activated by autophosphorylation (41). PDGF treatment of HSCs leads to FAK phosphorylation that is blocked by a dominant-negative form of Ras (42). Using a novel approach with an adenovirus expressing a dominant-negative form of FAK, FAK-CD, we

A.

B.
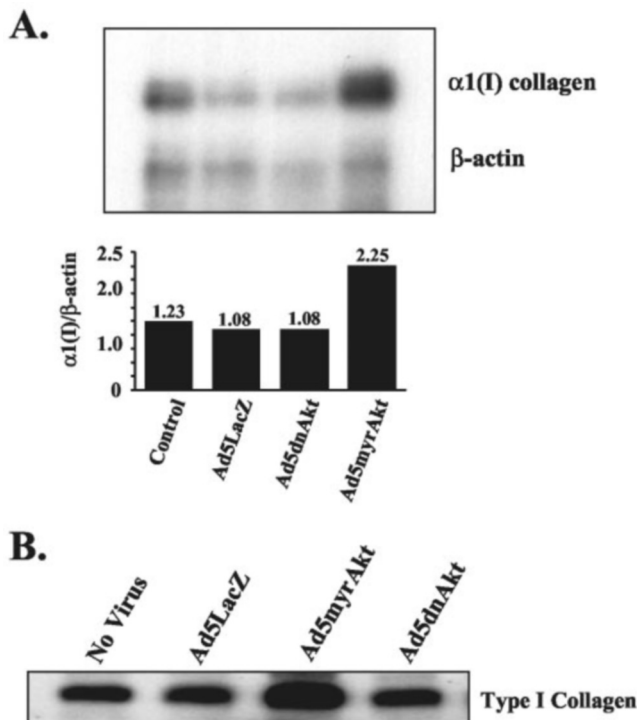
FIG. 11. **Akt stimulates $\alpha1(I)$ collagen mRNA and type I collagen protein expression.** *A*, culture-activated HSCs were transduced at m.o.i. = 500 with Ad5LacZ, Ad5dnAkt, or Ad5myrAkt. Total RNA was isolated 7 days after transduction, and RNase protection assays were performed for $\alpha1(I)$ collagen and β-actin mRNA, which was used as an internal control. Expression of $\alpha1(I)$ collagen mRNA is graphically expressed relative to β-actin (*lower panel*). *B*, culture-activated HSCs were left untreated or transduced with Ad5LacZ, Ad5myrAkt, or Ad5dnAkt. After 7 days of infection in growth conditions, total cell proteins were harvested, and Western blot analysis was performed for type I collagen. Equal loading of the gel was confirmed by Ponceau S staining of the transfer membrane (data not shown).
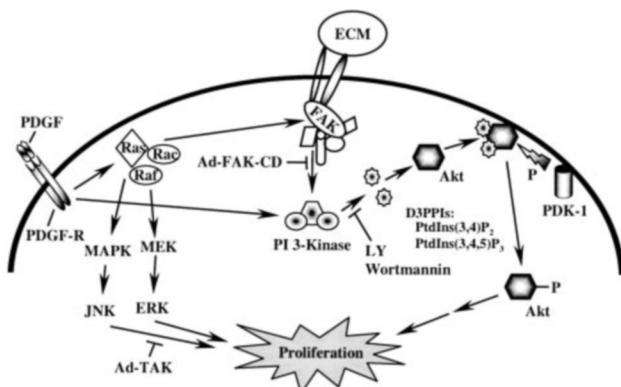
FIG. 12. **Proliferative signaling pathways in HSCs.** *PDGF-R*, PDGF receptor; *ECM*, extracellular matrix; *PDK-1*, phosphoinositide-dependent kinase-1; *D3PPIs*, D3-phosphorylated phosphoinositols; *PtdIns*, phosphatidylinositol; *LY*, LY294002; *TAK*, transforming growth factor-β-activated kinase-1.

have shown that PDGF treatment activates and requires FAK and Akt, a downstream target of FAK, for PDGF-induced HSC proliferation as assessed by [3H]thymidine incorporation. We also showed that FAK is positioned upstream of PI3K and Akt in the proliferative response based on PI3K activity and the phosphorylation status of Akt. FAK-CD overexpression also results in decreased DNA synthesis in endothelial cells (11). Overexpression of wild-type FAK increases cyclin D1 expression, decreases p21 expression, and accelerates G_1-to-S phase transition in NIH3T3 cells (43). Overexpression of dominant-

negative FAK blocks cyclin D1 up-regulation, induces p21 expression, and inhibits DNA synthesis in human foreskin fibroblast cells (43). Our data demonstrate that FAK plays a role in DNA synthesis and cell proliferation in activated HSCs.

Integrin signaling through FAK has a role in regulating cell spreading, migration, and proliferation. Cultured fibroblasts isolated from FAK null mouse embryos, which demonstrate a lethal phenotype, show reduced cell motility (28). Overexpressing a dominant-negative form of FAK decreases cell spreading and migration in endothelial umbilical vein cells (11). Similarly, we demonstrated that inhibiting FAK blocks HSC migration. A role of FAK in cell adhesion has not been well established. Cultured $FAK^{-/-}$ cells do not show altered adhesion to fibronectin (28). Overexpressing FAK in Chinese hamster ovary cells has no effect on cell adhesion (44). However, it was recently demonstrated that FAK is required for attachment of a human melanoma cell line (45). We showed that FAK is required for attachment of activated HSCs. Therefore, activated HSCs show a similar requirement of FAK for cell attachment as shown in other nontransformed cells.

The PI3K-Akt pathway is also activated following PDGF stimulation of HSCs (13). Akt can be activated not only by growth factors that trigger tyrosine kinase activity or activation of cytokine receptors, but also by other signals that activate PI3K, including integrins, thus linking FAK activation to this signaling pathway (18, 20). Activated Akt is a key downstream survival factor that stimulates cell proliferation and inhibits apoptosis (31, 46, 47). Our studies confirm that activation of PI3K is important for HSC proliferation and chemotaxis (13). A role for PI3K in HSC proliferation is supported by *in vivo* studies showing that, in rats, CCl_4 treatment leads to autophosphorylation of the PDGF receptor and increased PI3K activity. Furthermore, inhibition of PI3K by wortmannin blocks mitogenesis in response to PDGF, supporting the involvement of this pathway in HSC proliferation (13). We and others have shown similar results in HSC proliferation using a more specific PI3K inhibitor, LY294002 (32). However, we provide additional support showing that the phosphorylation of Akt at Ser[473] is induced by serum or PDGF and is inhibited by LY294002 and that this inhibits cell proliferation. Inhibition of PI3K with wortmannin also reduces ERK activity and c-Fos mRNA levels, suggesting that cross-talk occurs between the PI3K and MAPK pathways following PDGF stimulation in HSCs (34). The phosphorylation status of Akt correlated with an increase in HSC proliferation, $\alpha1(I)$ collagen mRNA levels, and type I collagen protein levels, demonstrating a regulatory role of Akt in these processes. Inhibition of both PI3K with LY294002 and Akt by adenovirus-mediated transduction of a dominant-negative form of Akt markedly reduced HSC proliferation. Transduction of HSCs with an adenovirus expressing a constitutively active form of Akt induced HSC proliferation in low serum conditions, thereby demonstrating that Akt is positioned downstream of PI3K and reaffirming its role in HSC proliferation.

TGF-β, the most potent fibrogenic cytokine in the HSC, did not induce Akt phosphorylation in the HSC. This might be related to the antiproliferative property of TGF-β in HSCs (30). TGF-β failed to block Akt activation by PDGF when administered prior to, at the same time as, or following PDGF treatment. These results are similar to those of Chen *et al.* (48), who found that suppression of the antiproliferative effect of TGF-β in human hepatoma cells (Hep3B) is dependent on the PI3K-Akt pathway. This suggests that PDGF, as found in our study, may impair the antiproliferative effect of TGF-β.

HSC activation produces a dramatic induction of type I collagen gene expression. We show here that PI3K is important in

regulating $\alpha1(I)$ collagen gene expression. Inhibition of PI3K with LY294002 or Akt by adenovirus-mediated transduction of a dominant-negative form of Akt markedly reduced $\alpha1(I)$ collagen mRNA and type I collagen protein levels. Blocking PI3K with LY294002 inhibited collagen expression at both the mRNA and protein levels, similar to previously reported observations in lung fibroblasts (49). However, mRNA levels in HSCs decreased at a much slower rate than in lung fibroblast cells. This may reflect different half-lives of the $\alpha1(I)$ collagen mRNA in the two cell types. Increased stability of $\alpha1(I)$ collagen mRNA occurs following HSC activation mediated through protein interactions within the 3′-untranslated region of the mRNA molecule and is an important mechanism for controlling $\alpha1(I)$ collagen gene expression in the HSC (50, 51). Interestingly, extracellular collagen protein levels were significantly reduced within 24 h after inhibiting PI3K activity, whereas the intracellular unprocessed collagen levels remained essentially unchanged even after 72 h of treatment. This may reflect an inhibition of collagen secretion following LY294002 treatment with an accumulation of unprocessed intracellular collagen. Because collagenase activity is primarily found extracellularly, there may be no mechanism to degrade the unprocessed intracellular collagen.

In summary, we have shown that the FAK-PI3K-Akt signaling pathway is a critical pathway for PDGF-induce HSC proliferation. Fig. 12 represents current knowledge for intracellular signaling leading to HSC proliferation. In addition, we have demonstrated that PI3K is an important modulator of $\alpha1(I)$ collagen gene expression. Together, this information indicates that this signaling pathway may provide a potential therapeutic target to modulate the fibrogenic response in the liver.

REFERENCES

1. Friedman, S. L. (2000) *J. Biol. Chem.* **275,** 2247–2250
2. Eng, F. J., and Friedman, S. L. (2000) *Am. J. Physiol.* **279,** G7–G11
3. Maher, J. J., Bissell, D. M., Friedman, S. L., and Roll, F. J. (1988) *J. Clin. Invest.* **82,** 450–459
4. Friedman, S. L., Rockey, D. C., McGuire, R. F., Maher, J. J., Boyles, J. K., and Yamasaki, G. (1992) *Hepatology* **15,** 234–243
5. Knittel, T., Schuppan, D., Meyer zum Buschenfelde, K.-H., and Ramadori, G. (1992) *Gastroenterology* **102,** 1721–1735
6. Pinzani, M., Marra, F., and Carloni, V. (1998) *Liver* **18,** 2–13
7. Claesson-Welsh, L. (1994) *J. Biol. Chem.* **269,** 32023–32026
8. Friedman, S. L., and Authur, M. J. P. (1989) *J. Clin. Invest.* **84,** 1780–1785
9. Pinzani, M., Gesualdo, L., Sabbah, G. M., and Abboud, H. E. (1989) *J. Clin. Invest.* **8,** 1786–1793
10. Marshall, C. J. (1995) *Cell* **80,** 179–185
11. Gilmore, A. P., and Romer, L. H. (1996) *Mol. Biol. Cell* **7,** 1209–1224
12. Carloni, V., Pinzani, M., Giusti, S., Romanelli, R. G., Parola, M., Bellomo, G., Failli, P., Hamilton, A. D., Sebti, S. M., Laffi, G., and Gentilini, P. (2000) *Hepatology* **31,** 131–140
13. Marra, F., Gentilini, A., Pinzani, M., Choudhury, G. G., Parola, M., Herbst, H., Dianzani, M. U., Laffi, G., Abboud, H. E., and Gentilini, P. (1997) *Gastroenterology* **112,** 1297–1306
14. Chen, H.-C., and Guan, J.-L. (1994) *J. Biol. Chem.* **269,** 31229–31233
15. Richardson, A., Malik, R. K., Hildebrand, J. D., and Parsons, J. T. (1997) *Mol. Cell. Biol.* **17,** 6906–6914
16. Parker, P. J., and Waterfield, M. D. (1992) *Cell Growth Differ.* **3,** 747–752
17. Chan, T. O., Rittenhouse, S. E., and Tsichlis, P. N. (1999) *Annu. Rev. Biochem.* **8,** 965–1014
18. Khwaja, A., Rodriguez-Viciana, P., Wennstrom, S., Warne, P. H., and Downward, J. (1997) *EMBO J.* **16,** 2783–2793
19. Shaw, M., Cohen, P., and Alessi, D. R. (1998) *Biochem. J.* **336,** 241–246
20. King, W. G., Mattaliano, M. D., Chan, T. O., Tsichlis, P. N., and Brugge, J. S. (1997) *Mol. Cell. Biol.* **17,** 4406–4418
21. Muraga, C., Fukuhara, S., and Gutkind, J. S. (1995) *J. Biol. Chem.* **275,** 12069–12073
22. Rippe, R. A., Almounajed, G., and Brenner, D. A. (1995) *Hepatology* **22,** 241–251
23. Xu, L.-H., Yang, X., Bradham, C. A., Brenner, D. A., Baldwin, A. S., Jr., Craven, R. J., and Cance, W. G. (2000) *J. Biol. Chem.* **275,** 30597–30604
24. Romashkova, J. A., and Makarov, S. S. (1999) *Nature* **401,** 86–90
25. Kotani, K., Ogawa, W., Hino, Y., Kitamura, T., Ueno, H., Sano, W., Sutherland, C., Granner, D. K., and Kasuga, M. (1999) *J. Biol. Chem.* **274,** 21305–21312
26. Rosenberg, I. M., Goke, M., Kanai, M., Reinecker, H. C., and Podolsky, D. K. (1997) *Am. J. Physiol.* **273,** G824–G832
27. Rivera, C. A., Bradford, B. U., Hunt, K. J., Adachi, Y., Schrum, L. W., Koop, D. R., Burchardt, E.-R., Rippe, R., and Thurman, R. G. (2001) *Am. J. Physiol.* **281,** G200–G207
28. Ilic, D., Furuta, Y., Kanazawa, S., Takeda, N., Takeda, N., and Sobue, K. (1995) *Nature* **377,** 539–544
29. Bachem, M. G., Riess, U., and Gressner, A. M. (1989) *Biochem. Biophys. Res. Commun.* **162,** 708–714
30. Saile, B., Mathes, N., Knittel, T., and Ramadori, G. (1999) *Hepatology* **30,** 196–202
31. Madge, L. A., and Pober, J. S. (2000) *J. Biol. Chem.* **275,** 15458–15465
32. Gentilini, A., Marra, F., Gentilini, P., and Pinzani, M. (2000) *J. Hepatol.* **32,** 227–234
33. Marra, F., Arrighi, M. C., Fazi, M., Caligiuri, A., Pinzani, M., Romanelli, R. G., Efsen, E., Laffi, G., and Gentilini, P. (1999) *Hepatology* **30,** 951–958
34. Marra, F., Pinzani, M., DeFranco, R., Laffi, G., and Gentilini, P. (1995) *FEBS Lett.* **376,** 141–145
35. Marra, F., Choudhury, G. G., Abboud, H. E., Reeves, H. L., Thompson, M. G., Dack, C. L., Burt, A. D., and Day, C. P. (1996) *J. Clin. Invest.* **98,** 1218–1230
36. Mitsui, H., Takuwa, N., Kurokawa, K., Exton, J. H., and Takuwa, Y. (1997) *J. Biol. Chem.* **272,** 4904–4910
37. Bost, F., McKay, R., Dean, N., and Mercola, D. (1997) *J. Biol. Chem.* **272,** 33422–33429
38. Schnabl, B., Bradham, C. A., Bennett, B. L., Manning, A. M., Stefanovic, B., and Brenner, D. A. (2001) *Hepatology* **34,** 953–963
39. Lavoie, J. N., L'Allemain, G., Brunet, A., Muller, R., and Pouyssegur, J. (1996) *J. Biol. Chem.* **271,** 20608–20616
40. Kawada, N., Ikeda, K., Seki, S., and Kuroki, T. (1999) *J. Hepatol.* **30,** 1057–1064
41. Kornberg, L., Earp, H. S., Parsons, J. T., Schaller, M., and Juliano, R. L. (1992) *J. Biol. Chem.* **267,** 23439–23442
42. Carloni, V., Pinzani, M., Giusti, S., Romanelli, R. G., Parola, M., Bellomo, G., Failli, P., Hamilton, A. D., Sebti, S. M., Laffi, G., and Gentilini, P. (1999) *J. Cell Biol.* **147,** 611–618
43. Zhao, J. H., Reiske, H., and Guan, J.-L. (1998) *J. Cell Biol.* **143,** 1997–2008
44. Cary, L. A., Chang, J. F., and Guan, J.-L. (1996) *J. Cell Sci.* **109,** 1787–1794
45. Maung, K., Easty, D. J., Hill, S. P., and Bennett, D. C. (1999) *Oncogene* **18,** 6824–6828
46. Kim, A. L., Khursigara, G., Sun, X., Franke, T. F., and Chao, M. V. (2001) *Mol. Cell. Biol.* **21,** 893–901
47. Bulik, G., Klippel, A., and Weber, M. J. (1997) *Mol. Cell. Biol.* **17,** 1595–1606
48. Chen, R. H., Su, Y. H., Chuang, R. L., and Chang, T. Y. (1998) *Oncogene* **17,** 1959–1968
49. Ricupero, D. A., Poliks, C. F., Rishikof, D. C., Cuttle, K. A., Kuang, P.-P., and Goldstein, R. H. (2001) *Am. J. Physiol.* **281,** C99–C105
50. Stefanovic, B., Hellerbrand, C., and Brenner, D. A. (1995) *Nucleic Acids Symp. Ser.* **33,** 212–214
51. Lindquist, J. N., Marzluff, W. F., and Stefanovic, B. (2000) *Am. J. Physiol.* **279,** G471–G476